**Biophysical Journal, Volume *116***

## Supplemental Information

# Anomalous Diffusion in Inverted Variable-Lengthscale Fluorescence Correlation Spectroscopy

**Michael D.N. Stolle and Cécile Fradin**

# Anomalous diffusion in inverted variable-lengthscale fluorescence correlation spectroscopy

Michael Stolle and Cécile Fradin

# Supplementary information

## 1. Autocorrelation function calculation

### 1a. Time-averaged autocorrelation function

By definition, the autocorrelation function (ACF) of a signal $F(t)$ is:

$$G(\tau) = \frac{\langle F(t)F(t+\tau)\rangle}{\langle F(t)\rangle^2} - 1, \qquad \text{SI Eq. 1}$$

where the brackets usually denote temporal averaging.

The numerator in SI Eq. 1 is a convolution, and the convolution of any two functions $x(t)$ and $y(t)$ can be rewritten as the inverse Fourier transform of the product of $\tilde{x}(k)$ and $\tilde{y}(k)$, the Fourier transforms of $x(t)$ and $y(t)$:

$$\int_{-\infty}^{+\infty} x(t)y(t+\tau)dt = \int_{-\infty}^{\infty} e^{-ikt}\tilde{x}(k)\tilde{y}(k)dk.$$

As a result of our simulations, we obtain for each observation volume size a discrete list of $M$ intensities, $F(s\Delta t)$. Here $\Delta t$ is the time interval between two recordings of the intensity, and $s$ is an integer which can take any value between 0 and $M$. The temporal averaging of the signal was then done with a discrete sum, using symmetric normalization to improve accuracy at large lag-times (1,2):

$$G(m\Delta t) = \frac{(M-m)\sum_{k=1}^{M-m} F(k\Delta t)F((k+m)\Delta t)}{\sum_{k=1}^{M-m} F(k\Delta t)\sum_{k=1}^{M-m} F((k+m)\Delta t)} - 1. \qquad \text{SI Eq. 2}$$

In order to save computation time when calculating the numerator in SI Eq. 2, which is a discrete convolution over a limited time range, we used a Discrete Fourier transform (DFT). The Fourier transform of the signal was thus calculated as:

$$F_k = \frac{1}{M+1}\sum_{n=0}^{M} F(n\Delta t)e^{\frac{2ikn}{M+1}}. \qquad \text{SI Eq. 3}$$

In order to avoid aliasing due to the DFT producing a periodic function of length $M$, the time domain of the data was zero-padded so that $F(n\Delta t)$ had a length of $2N$.

The denominator in SI Eq. 2 was calculated directly from the intensity data for each value of $m$, after which $G(m\Delta t)$ was straightforwardly calculated by dividing the numerator by the denominator.

**1b. Ensemble-averaged autocorrelation function**

In some cases (for the CTRW model), in order to test the ergodicity of the diffusion process, a second ACF was calculated, by performing an ensemble average instead of a time average. In this case, a separate intensity trace, $F_j(s\Delta t)$, was generated for each of $N$ particles (with j = 1 to N, and $N = 3200000$). The ensemble averaged ACF was then calculated (without performing a Fourier transform) as:

$$G(m\Delta t) = \frac{N\sum_{j=1}^{N} F_j(0)F_j(m\Delta t)}{\sum_{j=1}^{N} F_j(0)\sum_{j=1}^{N} F_j(m\Delta t)} - 1. \qquad \text{SI Eq. 4}$$


1. Schätzel, K., M. Drelle, and Stimac, 1988. Photon correlation measurements at large lag times: improving statistical accuracy. Journal of Modern Optics 35:711-718.
2. Shi, X. And T. Wohland, 2010. Fluorescence correlation spectroscopy. In Diaspro, editor, Nanoscopy and multidimensional optical fluorescence microscopy, CRC press.

## 2. Stick-and-diffuse model

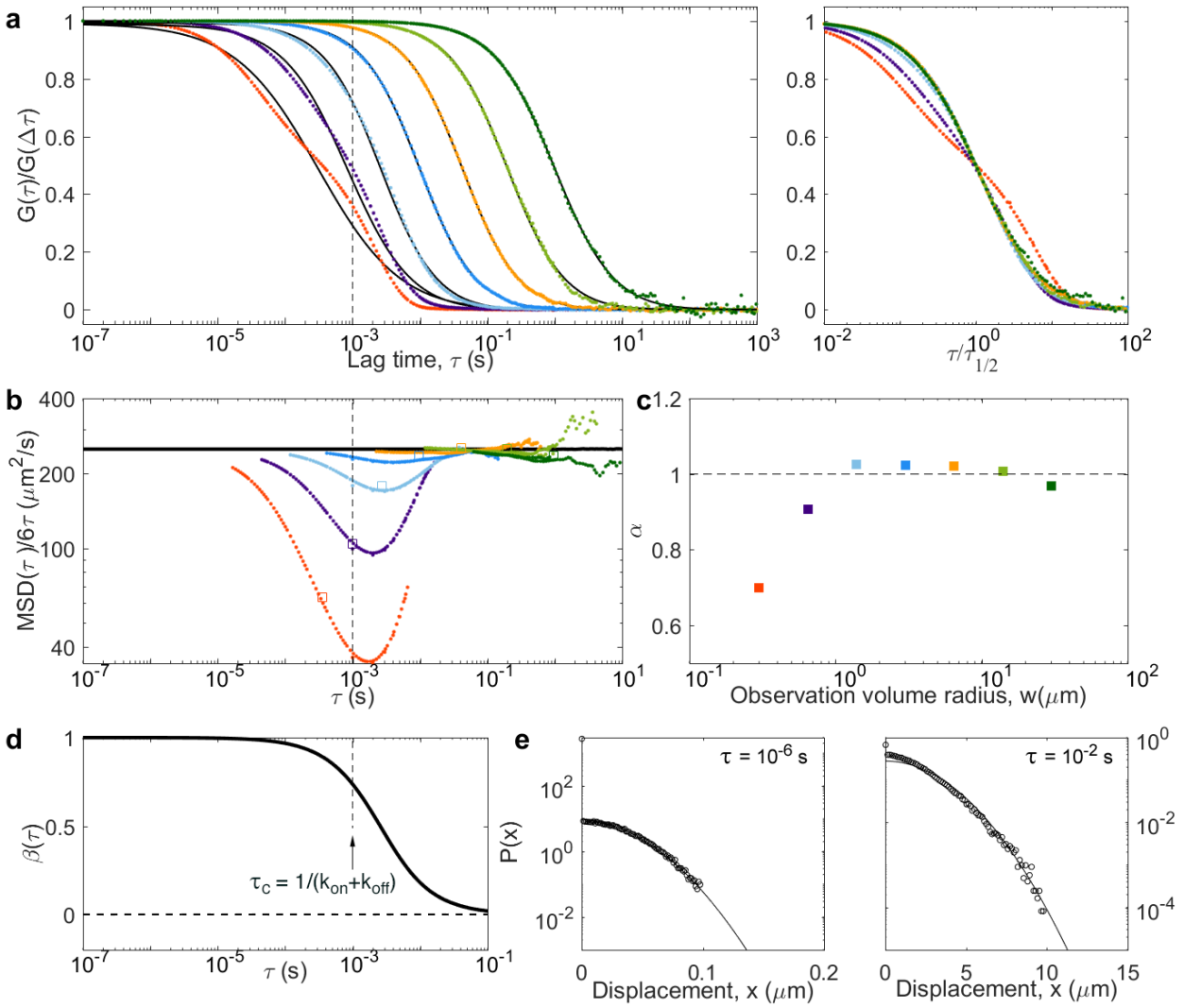


**Fig. 1.** Two-component diffusion with D = 500 μm²/s and D' = 0 μm²/s (corresponding to the stick-and-diffuse model). Panels are as in Figs. 5-11 in the main text: (a) ACFs, (b) MSDs, (c) anomalous exponent (d) non-Gaussian parameter, (e) distribution of displacements. The transition rates were $k_{on} = k_{off} = 500$ s$^{-1}$, thus f = 0.5. Then $D_{avg} = 250$ μm²/s, $D_\infty = 0$ μm²/s, and $\beta = 1$ at small $\tau$. The characteristic time is $\tau_c = 1$ ms, corresponding to $w_c \sim 1$ μm.

### 3. Diffusion in impermeable cages

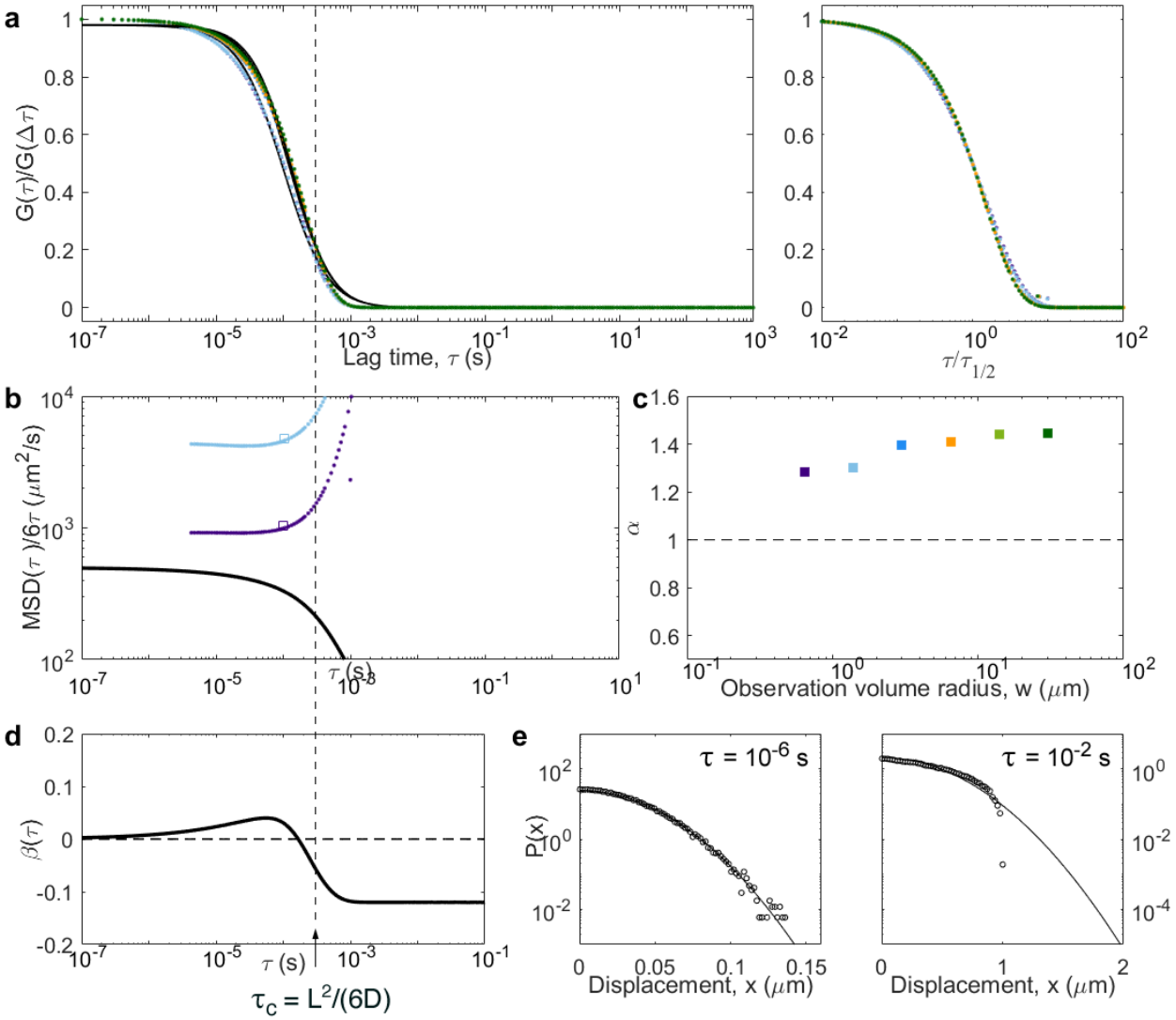


**Fig. 2.** Caged diffusion with D = 500 μm²/s, L = 1 μm and p = 0, corresponding to a case where the cages are completely impermeable. Panels are as in Figs. 5-11 in the main text. The ACFs converge very quickly to a form that has a very sharp decay ($\alpha$ ~1.4), with a characteristic decay time depending on the size of the cages rather than the size of the observation volume, and connected to the cage relaxation time, $\tau_c = L^2/6D = 0.33$ ms here.

**4. Effect of photon noise on the inverted ACFs**

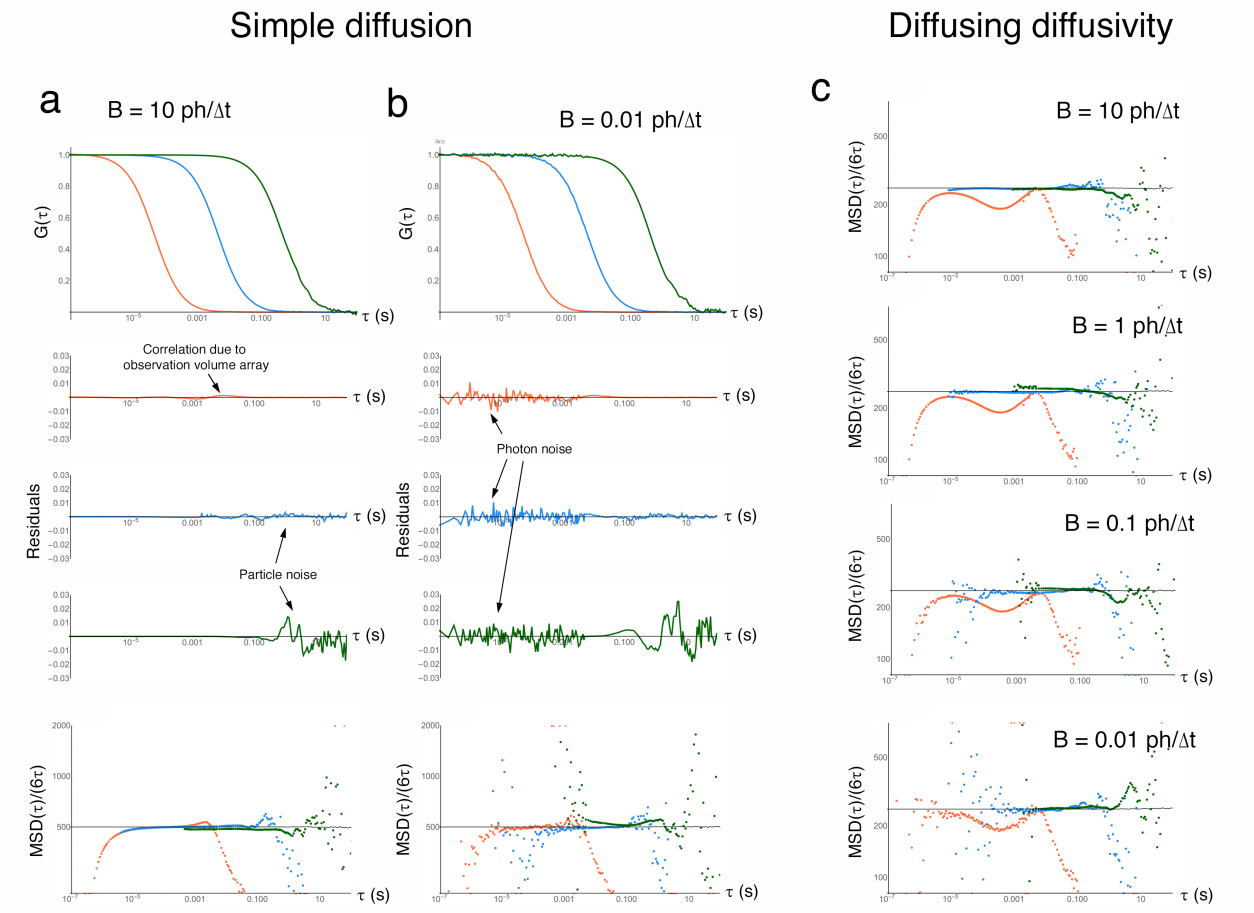


**Fig. 3.** Effect of photon noise on the inversion of the ACFs. All the simulations presented in this figure were done taking into account photon noise, i.e. drawing the value of the intensity for each $\Delta t = 10^{-7} s$ time bin from a Poisson distribution with average value calculated using Eq. 14 in the main text. **(a,b)** Result of simulations done for particles undergoing simple diffusion (same parameters as in Fig. 4 in the main text), with a molecular brightness $B$ = 10 photons/time bin (a) or $B$ = 0.01 photons/time bin. The upper panels show the ACFs obtained for $w = 0.3 \mu m$ (red curve), $w = 3 \mu m$ (blue curve) and $w = 30 \mu m$ (green curve), each normalized to the average of the first 5 points of the ACF. The three middle panels show the residuals obtained when fitting the ACF with a simple diffusion model. The lower panels show the inverted and normalized ACFs (the black curve shows the actual MSD as calculated from the trajectories). Note that a larger range of inverted data is shown here (compared to the results shown in the main text), to better show the limits of the useful inversion range. The effect of photon noise is visible for the lowest value of $B$, for lag times $\tau < 5 ms$, where the correlation is calculated using small $\Delta t = 10^{-7} s$ time bins, and by perturbing the proper normalization of the ACF it reduces the range of lag time (at short lag times) where the inversion procedure works. The photon noise is no longer visible for $\tau > 5 ms$ when larger $10^{-3} s$ time bins are used. With a multi-tau correlation scheme (rather than the 2-tau correlation scheme employed here), the photon noise would gradually decrease as $\tau$ increases. Particle noise is visible

for the larger observation volumes at long lag times. **(c)** Result of simulations performed for particles undergoing diffusing diffusivity (same parameters as in Fig. 9 in the main text), for different values of $B$, showing the gradual increase in statistical noise for the inverted ACFs as $B$ decreases. This increase in statistical photon noise is accompanied by a reduction of the range accessible for proper ACF inversion at short lag times. Despite this noise, the characteristic dip observed for the smallest observation volume is still clearly visible for $B$ = 0.01 photons/time bin.

**5. Effect of fluorophore photophysics on the inverted ACFs**

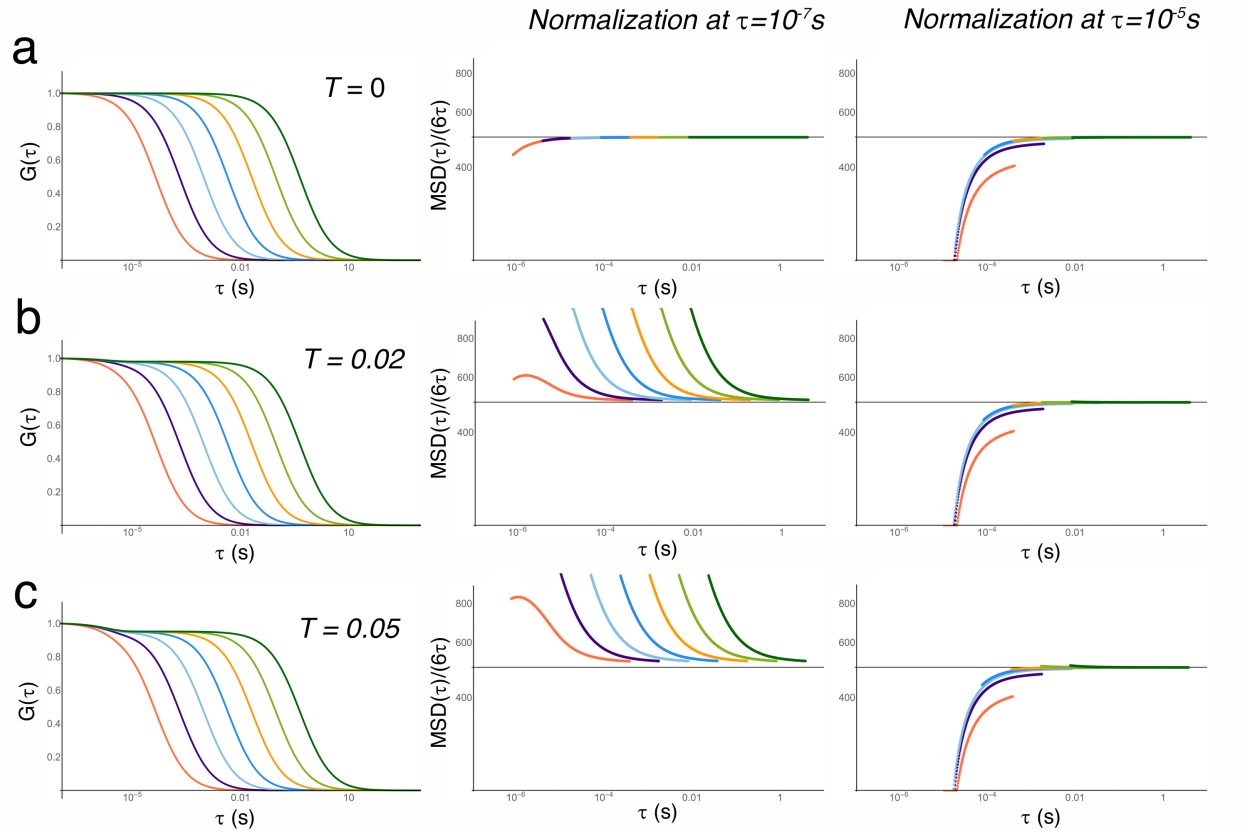


**Fig. 4.** Inversion of ACFs containing a photophysics term. ACFs for a range of detection volumes comprised between 0.3 and 30 µm were generated using the expression $G(\tau) = G_{SD}(\tau) \times (1 + T/(1-T)e^{-\tau/\tau_T})$, where $G_{SD}(\tau)$ is the form of the ACF for simple diffusion (Eq. 15 in the main text with $\alpha = 1$), $\tau_T$ is the triplet state relaxation time, and $T$ is the fraction of molecules in the triplet state. (a) T= 0, (b) $\tau_T = 2\mu s$ and $T = 0.02$, (c) $\tau_T = 2\mu s$ and $T = 0.05$. For each conditions, the calculated ACFs are shown in the left panel (normalized to the value of their first point), followed by the inverted ACFs using an average of the first 5 points of the ACF for normalization before the inversion (middle panel), and the by a second inversion using an average of 5 points around $\tau = 5\tau_T$ for the normalization instead (right panel). Although the inversion procedure is seriously affected when the ACF normalization is done at lag time around or below $\tau_T$, it is barely affected when the normalization is done for $\tau > 5\tau_T$. It is therefore possible to use the inversion procedure in the presence of photophysics, but

care has to be taken to normalize the ACF properly. A fitting of the photophysics term would yield even better results and allow to recover data for inversion below $5\tau_T$.

### 6. Effect of observation volume calibration errors on the inverted ACFs

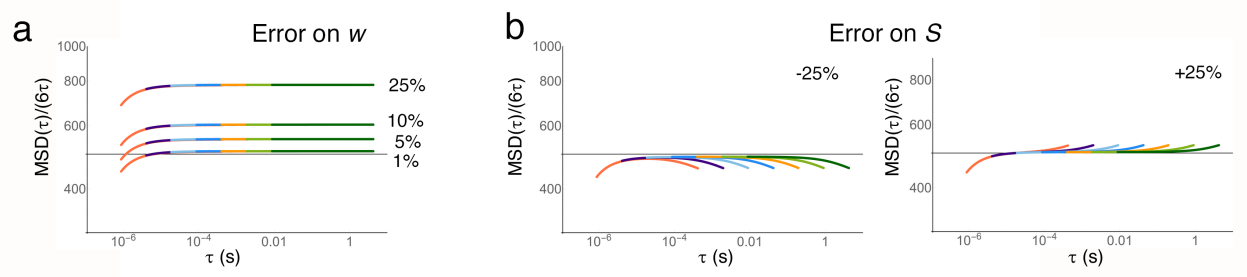


**Fig. 5.** Influence of calibration errors on the inverted ACFs. ACFs were first calculated for a range of detection volumes with $w$ comprised between 0.3 and 30 µm using Eq. 15 in the main text with $\alpha = 1$ (simple diffusion) and $S = 5$. The inversion was then performed using incorrect values for either $w$ or $S$ as an input (denoted as $w$' and $S$'). (a) Inverted ACFs (apparent MSD) obtained for values of $w'$ that were 1%, 5%, 10% and 25% larger than the actual values. The black line indicate the actual value of $MSD(\tau)/(6\tau)$. The inverted curves are shifted by a factor of $(w'/w)^2$ compared to this actual MSD. An error on $w$ therefore leads to an error on the estimate of the value of the diffusion coefficient (as it would in single point FCS), but not on the nature of the diffusion. (b) Inverted ACFs obtained for values of $S'$ that were either 25% higher or 25% lower than the actual value of $S$. The black line indicate the actual value of $MSD(\tau)/(6\tau)$. The inversion procedure is very robust against small (~10% or less) errors on the value of S, but for larger errors issues arise at long lag times (where $S$ influences the asymptotic behaviour of the ACF).